Density Measurements of a Free Jet by a Laser Differential Interferometer

By

Michio NISHIDA* and Akihiko NAKAJIMA*

(February 1, 1983)

Summary: In this paper a laser differential interferometer using Wollaston prisms was applied to the density measurements of an argon free jet and the radial density distributions at ten positions from an orifice were determined by using an Abel inversion under the assumption of an axisymmetric flow. From the measurements it was concluded that this method is effective to spatially resolve the density distributions of supersonic gas flows.

1. Introduction

Interferometry has been often used for density measurements. Most conventional ways using interferometry are such that the optical path change between a test beam and a reference beam caused by the density perturbation in a flow is observed as the fringe pattern on an interferogram. Therefore, quantitative measurements are difficult when the density perturbation becomes so small that the optical path change is less than an order of the light wave length.

The laser differential interferometer using Wollaston prisms developed by Smeets [1, 2] can resolve the optical path change up to about 1 per cent of the wave length. This interferometer has been widely applied to flow diagnostics. Smeets [3] measured the density distribution in the boundary layer using a multi-beam interferometer technique. The laser interferometry was also applied to the determination of the rotational relaxation time of D_2, using a cryogenic shock tube [4, 5]. This technique was employed for the diagnostics of reflected shock waves [6]. In the present work the laser differential interferometer was applied to the density measurements of an argon free jet expanding into a vacuum chamber through a sonic orifice and the spatially resolved density distributions were obtained by means of the Abel inversion.

2. Principle of Laser Interferometry

A schematic diagram of an optical system is shown in Fig. 1. The system is based on the same type of a laser differential interferometer as developed by Smeets [1]. The linear polarization of an original laser beam is transformed into a circular polarization by a $\lambda/4$ plate in order to be free from any orientation of the following Wollaston prism. The laser beam travels through the first Wollaston prism which is made of uniaxial birefringent crystal, and is split into two beams being perpen-

* Department of Aeronautical Engineering Kyoto University, Kyoto

This document is provided by JAXA.

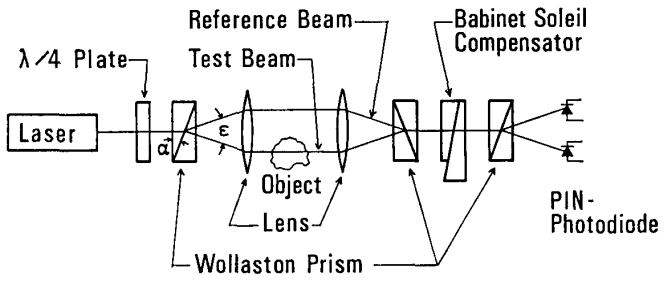

Fig. 1. Optical system for laser differential interferometry.

dicularly polarized. A lens placed at the distance of its focal length from the Wollaston prism makes the two beams parallel. One of these beams works as a test beam; the other as a reference beam. The distance between the two beams can be set up arbitrarily by changing the focal length of the lens. The two partial beams pass through the test object, and an optical path change occurs between the two beams due to non-uniformity in the density. After passing through the second lens and the second Wollaston prism, the two beams are recombined and travel on the common path, but they don't interfere since they are still polarized perpendicularly. By a Babinet-Soleil compensator whose axes are aligned with the polarization directions, the relative phase difference between the beams which are polarized perpendicular to each other can be controlled.

When the polarization directions of the two partial beams entering into the last Wollaston prism are in the directions of the y- and z-axes, respectively, their optical disturbances are represented in the form

$$E_y=P_y\cos\left(\frac{2\pi x}{\lambda}\right),\qquad E_z=P_z\cos\left[\frac{2\pi}{\lambda}(x+\Delta\Phi)\right], \tag{1}$$

where x has been taken in the direction of the beam propagation, and y and z have been taken perpendicular to x, and $\Delta\Phi$ is the relative optical path difference between the two beams, λ the wave length, P_y and P_z the amplitudes of the beams. Finally, the partial beams are mixed by the third Wollaston prism whose axes are arranged 45° with respect to the polarization of the beams, and are split into two interfering pairs of beams. These two beams are received by two separate photodiodes. If their polarization directions are in the I- and II-directions, the beam intensities, I_{I} and I_{II}, are then expressed as

$$\begin{aligned} I_{\mathrm{I}}&=P_yP_z\cos\left(\frac{2\pi}{\lambda}\Delta\Phi\right)+\frac{1}{2}(P_y^2+P_z^2),\\ I_{\mathrm{II}}&=-P_yP_z\cos\left(\frac{2\pi}{\lambda}\Delta\Phi\right)+\frac{1}{2}(P_y^2+P_z^2). \end{aligned} \tag{2}$$

Thus the intensities vary as a function of the optical path difference. The beam intensities detected by PIN-photodiodes, which respond linearly over a wide range of the beam intensity, are converted to the voltages. The difference between two voltages, U, is written as

This document is provided by JAXA.

$$U=k_{\mathrm{I}}I_{\mathrm{I}}-k_{\mathrm{II}}I_{\mathrm{II}}=U_0\cos^2\left(\frac{\pi}{\lambda}\Delta\phi\right)+U_1 \qquad (3)$$

where $U_0=2(k_{\mathrm{I}}+k_{\mathrm{II}})P_yP_z$, $U_1=(1/2)k_{\mathrm{I}}(P_y-P_z)^2-(1/2)k_{\mathrm{II}}(P_y+P_z)^2$ and k_{I} and k_{II} are the constants to be determined from the PIN-photodiade performance and its circuit. Consequently, the change in the optical path difference is observed as a change in the voltage.

The density variation can be obtained from a variation of the output voltage. Let L be the width of the test section, n be the refractive index and let the subscripts 1 and 2 represent the conditions of the medium where the beams 1 and 2 travel. Then the optical path difference is given by

$$\frac{\Delta\Phi}{\lambda}=\frac{1}{\lambda}\left[\int_0^{L_2}n_2(x)dx-\int_0^{L_1}n_1(x)dx\right]. \qquad (4)$$

Since the Gladstone-Dale formula is expressed as $n-1=K\rho/\rho_0$, the relation between the density difference and the optical path difference is obtained as follows:

$$\frac{\Delta\Phi}{\lambda}=\frac{K}{\lambda\rho_0}\left[\int_0^{L_2}\rho_2(x)dx-\int_0^{L_1}\rho_1(x)dx\right], \qquad (5)$$

where ρ_0 is the density at the standard state (273 K, 1 atm), and K is the non-dimensional Gladstone-Dale constant for the standard stante. The relation between the output voltage U and the density difference $\Delta(\rho_2-\rho_1)$ is obtained from Eqs. (3) and (5),

$$U=U_0\cos^2\left[\frac{\pi K}{\lambda\rho_0}\int_0^{L}\Delta(\rho_2-\rho_1)dx\right]+U_1, \qquad (6)$$

where we have set $L_1=L_2=L$. For the argon gas the Gladstone-Dale constant is 2.94×10^{-4}. The relation between $\Delta\Phi/\lambda$ and U is shown in Fig. 2. In the center-part of the $\cos^2$-curve the output change ΔU is approximately expressed as

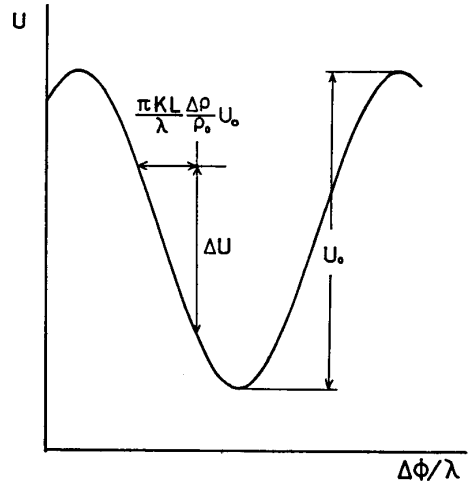

Fig. 2. Interference curve.

This document is provided by JAXA.

$$\frac{\Delta U}{U_0}=\frac{\pi K}{\lambda\rho_0}\int_0^L \Delta(\rho_2-\rho_1)dx. \qquad (7)$$

In order to obtain $\Delta\rho(=\Delta(\rho_2-\rho_1))$ from the experimental values of ΔU by using Eq. (7), the values of K, L, λ, ρ_0 and U_0 must be known. These values, except U_0, can be easily estimated. U_0 can be determined from the interference curve shown in Fig. 2, which has been obtained by using the Babinet-Soleil compensator. The initial optical path difference is also set up by means of this compensator.

3. Experimental Apparatus and Conditions

The laser differential interferometry method was applied to radial density measurements of an axisymmetric free jet expanding through an orifice (diameter D=5 mm) from a plenum chamber (9 cm in the diameter and 14.2 cm in the length) to a test chamber (27001). (cf. Fig. 3) The argon gas was used as a test gas. The experimental apparatus and the optical system are shown schematically in Fig. 4. The optical system is the same as shown in Fig. 1.

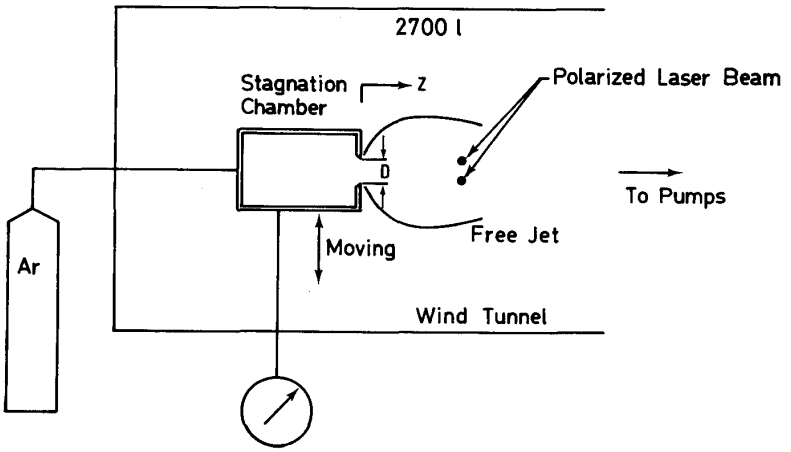

Fig. 3. Experimental apparatus.

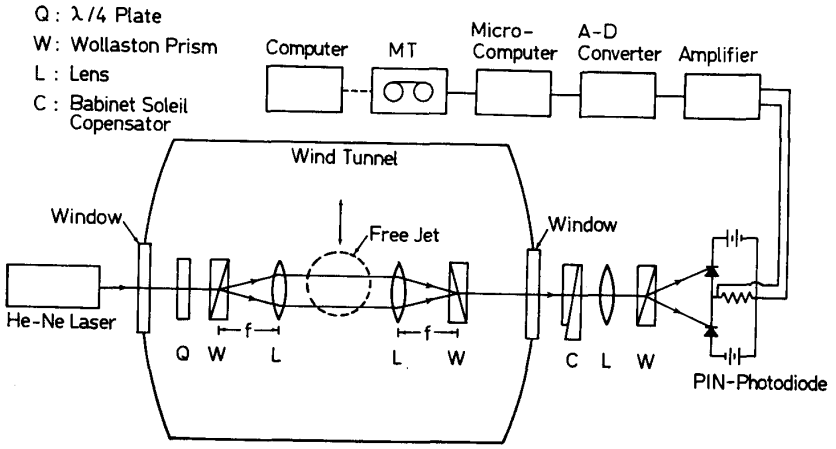

Fig. 4. Schematic diagram of experiment.

This document is provided by JAXA.

A linear polarized He–Ne laser (output power=25 mW, λ=632.8 nm) was used as a light source. The beam splitting angle of the Wollaston prism (calcite) was 3.9° and the distance between the two parallel beams in the test section was 13.6 mm. To avoid the perturbations caused by atmosphere convection on the optical path, the optical system where the beams are separated is set in the test chamber evacuated by pumps.

A lens placed between the Babinet-Soleil compensator and the third Wollaston prism focuses the beam on the photodiodes. Two PIN silicon photodiodes were used as detectors. The output voltages from the photodiodes are recorded on a magnetic tape (MT) controlled by a microcomputer. The data on the MT were analyzed on a large computer. Experimental conditions are as follows:

the stagnation pressure p_s=13.3 kPa (100 Torr)

the test chamber pressure p_∞=1.31 kPa (9.86 Torr)

Since the plenum chamber can be vertically moved so that the two beams can traverse the free jet, radial density distributions can be measured. The moving velocity of it is 100 mm/sec. The measurements were made at 10 locations between z=4 mm and 13 mm from the orifice.

4. Analysis of the Data

The measured data of the output change ΔU are shown in Fig. 5. This is the data obtained from the optical path change between the two beams having the width 13.6 mm. When the two beams travel in the ambient region, ΔU is taken to be zero. Fig. 6 shows the distribution of $\int \Delta\rho dx$, where $\Delta\rho=\rho-\rho_\infty$ (ρ_∞=the ambient density), obtained from Fig. 5. The result in Fig. 5 was obtained after low-pass-filtering (cut off frequency$\fallingdotseq$5 Hz) on the computer. $\Delta\rho$ can be easily estimated from the result on Fig. 5 as follows:

Since $R^2=y^2+(L/2)^2$ on Fig. 7, Eq. (7) is rewritten as

$$\frac{\Delta U}{U_0}=\frac{\pi K}{\lambda\rho_0}\int_0^{L(y)}\Delta\rho(r)dx=\frac{\pi K}{\lambda\rho_0}2\int_0^{\sqrt{R^2-y^2}}\Delta\rho(r)dx. \tag{8}$$

Now, assuming that $\Delta\rho(r)$ is expressed as a polynomial function of r and using the binomial theorem and the relation $r^2=x^2+y^2$ (see Fig. 7), we can write

$$\Delta\rho(r)=\sum_{n=0}^{N}a_n r^{2n}=\sum_{n=0}^{N}a_n(x^2+y^2)^n=\sum_{n=0}^{N}\left[a_n\sum_{m=0}^{n}\binom{n}{m}x^{2(n-m)}y^{2m}\right]. \tag{9}$$

Substituing Eq. (9) into Eq. (8), and integrating the resultant equation leads to

$$\frac{\Delta U(y)}{U_0}=\frac{2\pi K}{\lambda\rho_0}\sum_{n=0}^{N}\left[a_n\sum_{m=0}^{n}\binom{n}{m}\frac{1}{2n-2m+1}(R^2-y^2)^{n-m+(1/2)}y^{2m}\right]. \tag{10}$$

Since the measured values of ΔU are expressed as a function of y as shown in Fig. 7, the coefficients $a_0, a_1, a_2, \ldots, a_N$ can be easily determined by using Eq. (10). In the present work, $\Delta\rho$ was approximated as an even polynomial function of 40

This document is provided by JAXA.

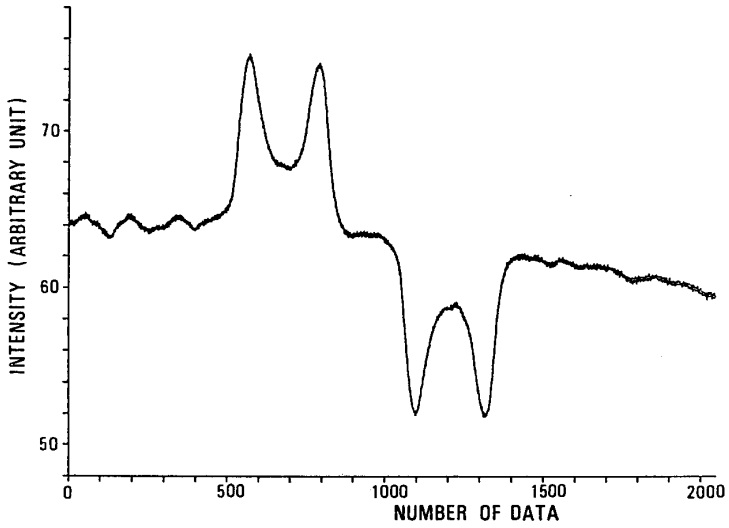

Fig. 5. Measured interference intensity (z=9 mm, p_s=13.3 kPa, p_∞=1.31 kPa).

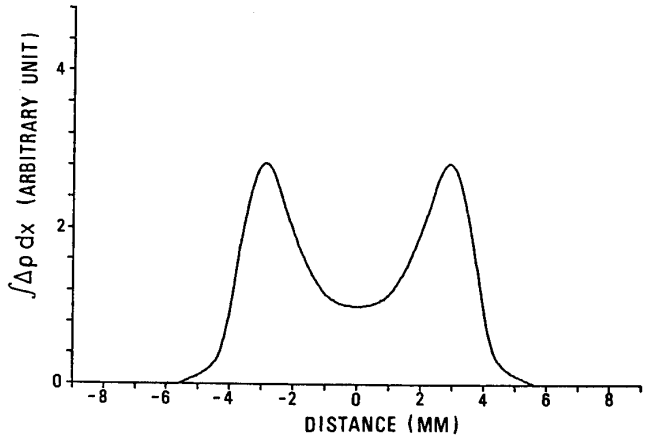

Fig. 6. Variation of $\int \Delta\rho dx$ in the y-direction (z=9 mm, p_s=13.3 kPa, p_s=1.31 kPa).

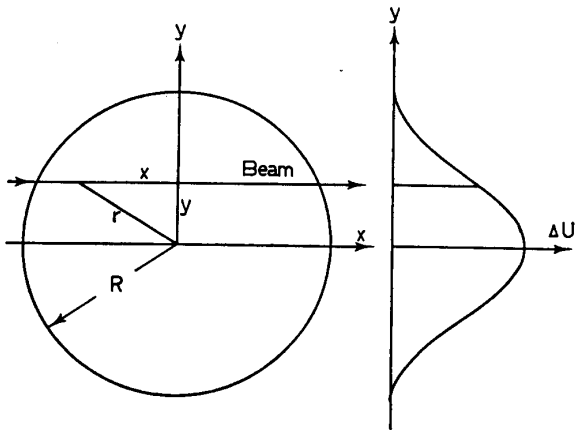

Fig. 7. Laser beam traversing freejet.

This document is provided by JAXA.

order so that 21 coefficients a_0, a_1, a_2, . . . , a_{20} were determined by using the method of least squares for about one thousand data of ΔU.

5. Results and Discussions

In Fig. 8 is shown the radial density distribution that has been obtained from the result on Fig. 7. The densities were normalized by the stagnation density ρ_s. The barrel shock can be observed on the both sides of the free jet. The disturbances at the foot of this distribution are recognized as the error of numerical calculations. In Fig. 9 is also shown the radial density distributions at 10 locations between $z=$ 4 mm($z/D=0.8$) and z=13 mm($z/D=2.6$). At $z/D=0.8$ a barrel shock is appreciably recognized, and at $z/D=1.0$ it develops more apparently. In the downstream of $z/D=2.2$, the density suddenly increases. That is caused by a compression due to a Mach disk. A comparison between the measured and predicted densities on the centerline of the free jet is shown in Fig. 10. The prediction was made by assuming the isentropically expanding free jet, where Mach numbers on the centerline were estimated from both the empirical relation given by Ashkenas and Sherman [7] and the measured impact pressure. A Mach disk position was predicted according to Ashkenas and Sherman [7]. The experimental density decreases toward the downstream in such a way as in the isentropic expansion. Also, the experimental Mach-disk position is in fairly good agreement with the predicted one.

From the present result, we may mention that the present method for measuring density can give a satisfactory radial distribution of the density for axisymmetric flows. Furthermore, if the present method is combined with the CT scan technique, it may be possible to determine local density at any section of non-axisymmetric flows.

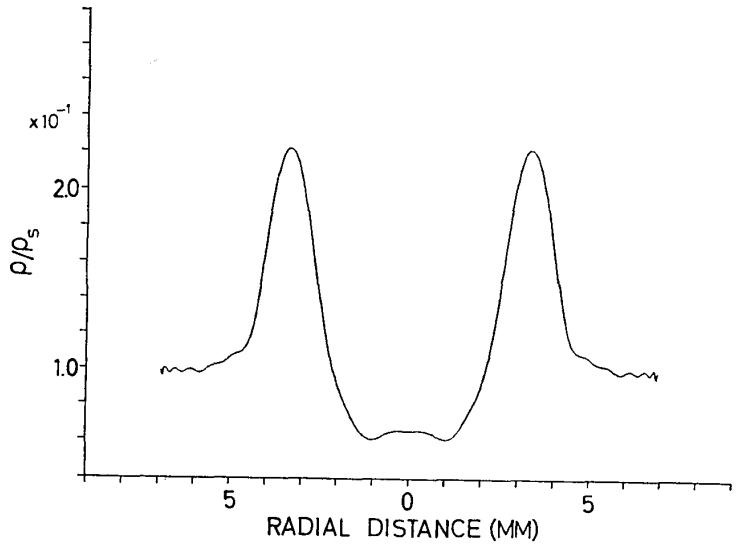

Fig, 8. Radial distribution of density ($z=9$ mm, $p_s=13.3$ kPa, $p_\infty=1{,}31$ kPa).

This document is provided by JAXA.

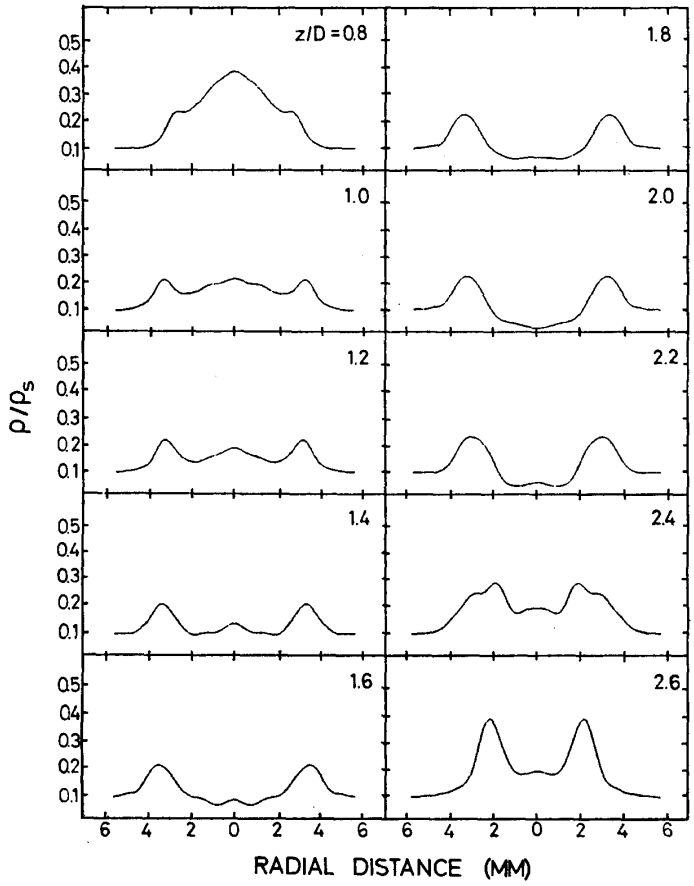

Fig. 9. Radial distributions of density at 10 locations between $z=4$ mm and $z=13$ mm from the orifice.

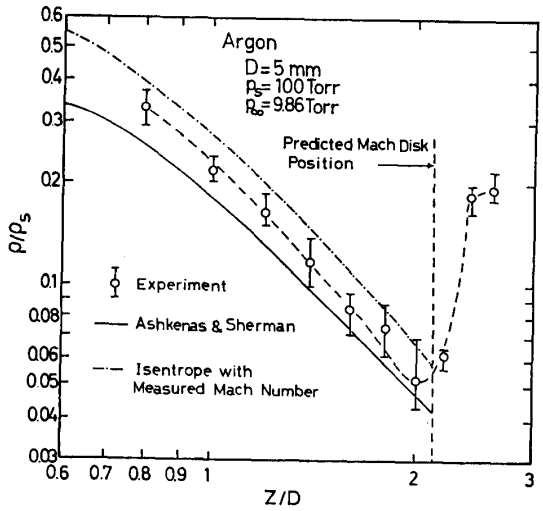

Fig. 10. Comparison of measured densities with predicted ones on the flow centerline.

Acknowledgment

This work was partially supported by the Ministry of Education (No. 56550046).

This document is provided by JAXA.

References

[1] G. Smeets: IEEE Transactions on Aerospace and Electronic System, Vol. 8, 186 (1972).
[2] G. Smeets: ibid Vol. 13, 82 (1977).
[3] G. Smeets: Proceedings of the 8th International Shock Tube Symposium, Chapman and Hall, London, 45 (1971).
[4] G. Lensch: Doctral Thesis, Technische Hochschule Aachen, Germany (1977).
[5] G. Lensch and H. Grönig: Shock Tube and Shock Wave Research, University of Washington Press, 132 (1978).
[6] W. Garen and G. Lensch: Shock Tubes and Waves, The Magnes Press, Jerusalem, 155 (1980).
[7] H. Ashkenas & F. S. Sherman: Rarefied Gas Dynamics, Academic Press, New York, Vol. 2, 84 (1965).

This document is provided by JAXA.